37
7-2-79
24 D NTIS

SAND79-0395
Unlimited Release

MASTER

Simulated Nuclear Optical Signatures Using Explosive Light Sources (ELS)*

Ronald F. Ginser


Sandia Laboratories

F 2900 Q(7-73)

DISTRIBUTION OF THIS DOCUMENT IS UNLIMITED

SAND79-0325
Unlimited Release
Printed May 1979

SIMULATED NUCLEAR OPTICAL SIGNATURES USING EXPLOSIVE LIGHT SOURCES (ELS)*

Ronald F. Glaser
Special Projects Division 1245
Sandia Laboratories
Albuquerque, NM 87185

ABSTRACT

Four Explosive Light Source (ELS) tests were conducted, simulating a nuclear optical waveshape. Visual observation was achieved at 25 km, line-of-sight bhangmeter detection at 10.5 km, and scattered-light detection at 1 km. The ELS would be a valuable training aid for Army troups.

NOTICE
This report was prepared as an account of work sponsored by the United States Government. Neither the United States nor the United States Department of Energy, nor any of their employees, nor any of their contractors, subcontractors, or their employees, makes any warranty, express or implied, or assumes any legal liability or responsibility for the accuracy, completeness or usefulness of any information, apparatus, product or process disclosed, or represents that its use would not infringe privately owned rights.

---

*Funding for the Nuclear Burst Detection System (NBDS) development and for participation in these Explosive Light Source (ELS) tests was provided by the United States Army Electronics Research and Development Command (USAERADCOM), Fort Monmouth, NJ under Project Number 76-09008.

DISTRIBUTION OF THIS DOCUMENT IS UNLIMITED

ACKNOWLEDGMENT

The author thanks John Dishon of Science Applications, Inc and Major Jim Mayo of the Defense Nuclear Agency for supplying the Explosive Light Sources; Terry Leighley, Clarence Robertson and Gene Moore of Sandia Laboratories for their photography; and Gary Laabs and his crew for Ground Zero support.

CONTENTS

ILLUSTRATIONS

ILLUSTRATIONS (cont)

TABLES

SUMMARY

Data gathered from ELS tests has indicated that:

- Clear air, line-of-sight optical transmission at ranges of from 0.3 to 10.5 km follows a $1/R^2$ dependance, allowing the ELS to be treated as a point source.

- From the large bags of the second pulse unit, light output scales as the number of bags to the two-thirds power, each bag yielding approximately 7 E7 Watts output.

- The proper timing of firing between the small and large bags permits simulation of a nulcear optical waveshape.

- The rise time of light from the first pulse is slower than that of a nuclear explosion, thereby limiting the range of detectability. When using NBDS sensors, their range is limited to 1 km while that of the direct line-of-sight bhangmeters (SSO, OSS) is 10.5 km.

- The ELS could be a valuable training aid for Army troops to emplace an NBDS system.

SIMULATED NUCLEAR OPTICAL SIGNATURES USING EXPLOSIVE LIGHT SOURCES (ELS)

Introduction

Four Explosive Light Source (ELS) tests were conducted on the test range at Sandia Laboratories in Albuquerque (SLA) from 28 February through 7 March 1978. The Appendix lists the participants and the fielded experiments. Although several types of measuring devices were used, this report documents only the optical time histories measured by the bhangmeters and the NBDS, and explains the conclusions reached. In general, the four shots made it possible to gather clear-air optical transmission data, determine the suitability of ELS to simulate the optical effects of a nuclear burst, and provide experience for the larger scale ELS tests to be conducted at Fort Ord, CA in April.

Explosive Light Source

The ELS is a mixture of aluminum powder and oxygen which, when detonated, produces extremely intense light and can be used to produce an optical time history that resembles a nuclear explosion (Figure 1). It also causes a large pulse of thermal radiation but little accompanying air blast. The ELS was developed and fielded by John Dishon of Science Applications Inc (SAI) under contract to the Defense Nuclear Agency (DNA).[1] It has been called "the world's largest flashbulb" because it uses the same general principle as an ordinary flashbulb, i.e., an envelope filled with oxygen in which aluminum is explosively burned (Figure 2). The intense light is produced in two pulses, each pulse generated with a different unit.

First Pulse Unit

The first pulse of maximum brillance in each shot was produced by an explosive system (E-system) consisting of 16 units, each containing four points. A point consisted of a detonator, a 6- to 8-in. piece of primer cord and a 2-g packet of aluminum powder encasing the end of the primer cord. The points were supported on PVC piping inside an envelope made of polyethelene bags 10 ft tall and 2 ft in diameter (Figure 3). The bags were inflated with oxygen just before detonation. All 64 points detonated almost simultaneously.

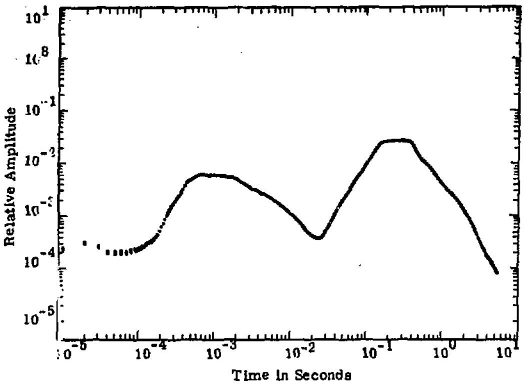

Figure 1

Nuclear Burst Optical Time History (Wideband Silicon Detector)

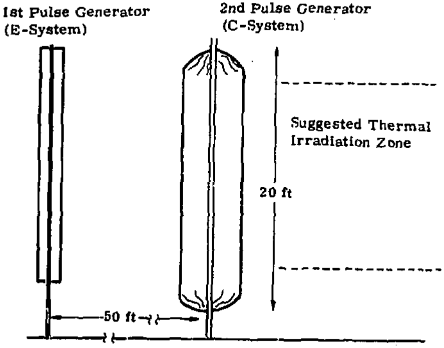

Side View of ELS Setup

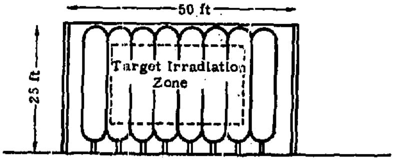

Back View of ELS Setup

Figure 2

Explosive Light Source Physical Setup

Figure 3. Explosive Light Source; 64-pt First Pulse System Before Inflating With Oxygen

Second Pulse Unit

The second pulse of maximum brillance in each shot was produced by a cannon system (C-system) consisting of eight bags or units. Each unit was composed of a polyethelene bag, 20 ft tall and 2 ft in diameter, filled with oxygen and containing a flare-type ignition device positioned approximately 3 ft from the bottom. Using pressurized nitrogen as the fluid, a fluidizing device at the base of each bag injected approximately 5 kg of aluminum powder past the flare which ignited it (Figure 4).

Figure 4. Explosive Light Source; 8-Bag Second Pulse System Before Inflating With Oxygen

Timing

Proper timing of aluminum injection and flare ignition in the second pulse unit in relation to the detonation of the first pulse system was mandatory to produce a simulated nuclear optical signature. Within limits, timing between units could be varied to simulate different nuclear yields.

Photo Detector Systems

Table I lists the photo detector systems (bhangmeters) used to measure the light and summarizes their characteristics. Briefly, there were two types of bhangmeters: unidirectional line-of-sight and omnidirectional scattered-light detectors (also called nuclear-burst detection system (NBDS) sensor stations). The former, of various vintages, different sensitivity, different sampled-time bases, etc, had to be aimed toward the source. The latter sensor is independent of azimuth and has a field-of-view (FOV) that is elevated above the horizon (source) to detect scattered light.

TABLE I

Bhangmeter Characteristics

Instrument	FOV	Trigger (W/cm^2)	Trigger Rate (W/cm^2-s)	Sensitivity (W/cm^2-V)	Saturation (V/cm^2)
Super Suitcase, Optical					
SSO A001 (LR) SSO A002 (LR)	5° Radius Direct	4 E-8	3.1 E-4	2 E-4	3.1 E-4
Old Style Suitcase (Former YSRM)					
OSS 1	12° Radius Direct	7.75 E-7	3 E-2	1 E-2	2.59 E-2
OSS 2 OSS 3	12° Semicircle Direct	7.75 E-9	3 E-2	1 E-4	2.59 E-4
Nuclear Burst Detection System Sensor Station					
NBDS A001 NBDS A002 NBDS A003	+4 to +10.5° 360° Azimuth Scattered	6.28 E-7	1.3 E-2	2 E-3	1.95 E-1

NOTE: All values assume no attenuating filters and silicon-peak wavelength response.

Super Suitcase Optical

The Super Suitcase Optical (SSO) (Figure 5) is an instrument that can measure the optical output as a function of time of light-producing phenomena. The system uses an unfiltered silicon photodiode sensor and digital samplers with variable time resolution. Figure 6 is a graph showing a typical broadband silicon detector response as a function of wavelength. The digital output levels are logarithmically spaced over six decades and the 200 digital sampling times are pseudologarithmically spaced over nine decades. A digital printer produces hard copy. Various triggering options can be selected with a switch and the gain of the optical detector may be increased by a factor of 140 for long range (LR) capabilities.

Figure 5. Super Suitcase Optical

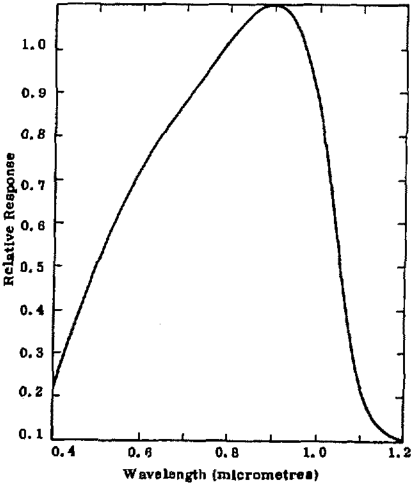

Figure 6. Broadband Silicon Response

Besides the digital record, a 16-mm color movie can be made with a camera mounted on the detector assembly. The FOV of the camera is closely matched and aligned with the optics of the detector to record the event alignment and weather conditions. Two SSOs were used for the ELS tests.[2]

Old Style Suitcase

The Old Style Suitcase (OSS) is an instrument that measures the optical time history of light-producing phenomena. The system uses an unfiltered silicon photodiode sensor and digital samples with variable time resolution. The 112 digital-output levels are logarithmically spaced over six decades; the 24 linearly spaced presamples and the 136 pseudo-logarithmically spaced main samples cover six decades. A digital printer provides hard copy output. Three OSSs were used during the ELS tests.

Nuclear Burst Detection System

The Nuclear Burst Detection System (NBDS) is normally an array of sensor stations (Figure 7) that detect and report characteristics of nuclear bursts, such as time of burst, yield, and ground interaction. To accomplish this, each sensor station uses a microprocessor to analyze the nuclear optical time history and the coincident arrival of an electromagnetic pulse (EMP) signal. Since the ELS does not produce an EMP, these requirements were bypassed with hard wiring. Each station obtains optical data using an unfiltered silicon photodiode sensor and digital samples with variable time resolution. The 256 digital-output levels are logarithmically spaced over six decades, and the 448 digital sampling times are pseudologarithmically spaced over 5-1/2 decades. In all cases but one on the first shot, the sensor stations were reprogrammed to function as independent instruments that measure the optical time history of any light-producing phenomena that meets threshold and rate-of-rise criteria. When programmed in this manner, each sensor station interfaces with a Silent 700 terminal that provides hard copy digital output. Three sensor stations were used during the ELS tests.

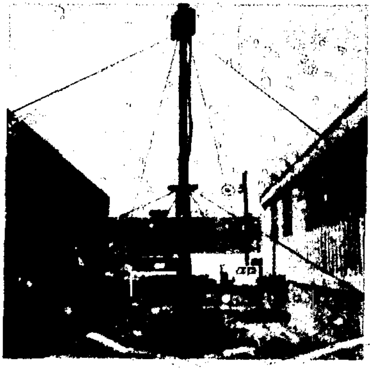

Figure 7

Tower-Mounted NBDS Sensor Station

Data

The bhangmeter data are organized by shot; Figures 8 and 9 are maps that show the locations of the detectors; Table II lists weather conditions reported at the Albuquerque airport; and Figure 10 (four parts) is a sequence of still photographs of an ELS shot. For size reference, the camera-protection shed shown in the foreground and to the left in Figure 10 was constructed of 4x8-ft plywood and asbestos sheets.

TABLE II

Weather Conditions

	Weather Time	Wind			Sky	Visibility
		Speed	Direction	Gusts		
Shot 1 2/28/78 16:34	15:54	6 knots (3.087 m/s)	150°	No	Overcast at 3000 ft (914 m)	40 miles (65 km)
Shot 2 3/2/78 11:20	10:55	12 knots (7.16 m/s)	230°	No	1/10 at 3000 ft (914 m) 6/10 at 10 000 (3048 m) 2/10 at 20 000 ft (6096 m)	60 miles (97 km)
Shot 3 3/3/78 13:40	13:00	8 knots (4.12 m/s)	30°	No	Overcast at 4000 ft (1219.2 m) Broken at 4500 ft (1371.6 m)	20 miles (32 km)
	14:00	7 knots (3.6 m/s)	0°	--	----	30 miles (48 km)
Shot 4 3/7/78 09:24	09:00	8 knots (4.12 m/s)	10°	No	2/10 at 5000 ft (1524 m) 2/10 at 12 000 ft (3657.6 m)	60 miles (97 km)

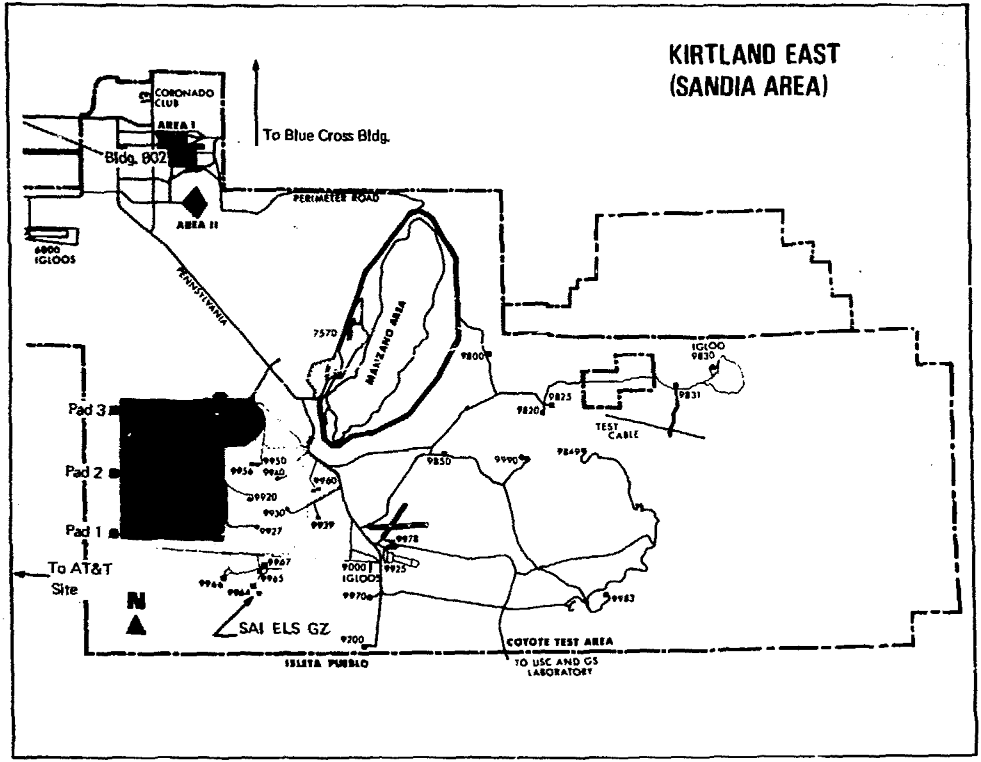

Figure 8. Kirtland East (Sandia Area)

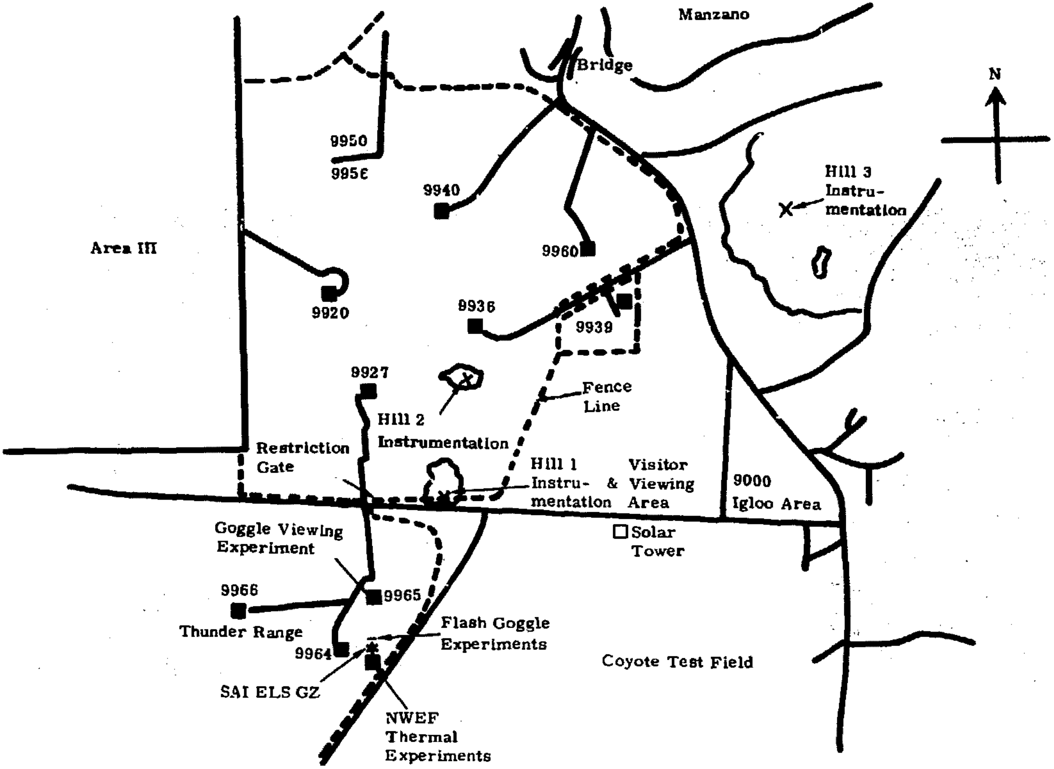

Figure 9. Coyote Test Field

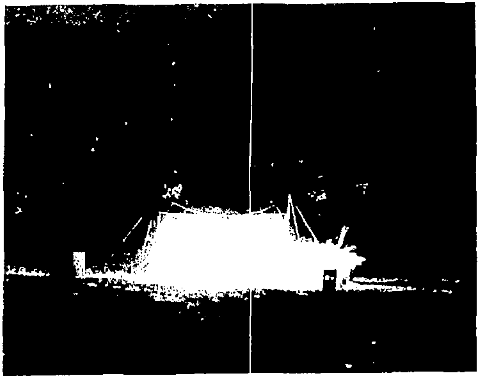

(a)

(b)

Figure 10. 8-Bag ELS

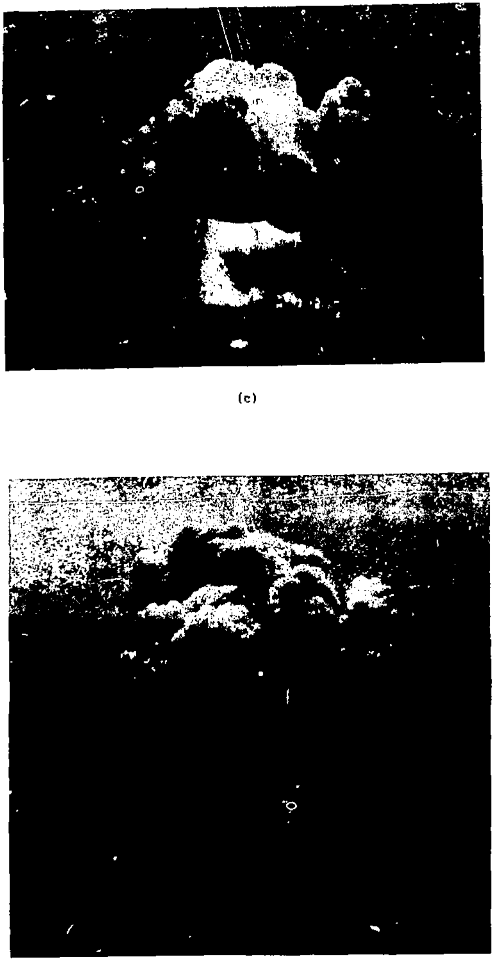

(c)

(d)

Figure 10. (concluded)

Shot 1

Table III summarizes bhangmeter data obtained from Shot 1. Optical time histories from four line-of-sight detectors at ranges from 1.0 to 10.5 km are plotted in Figure 11. This ELS produced optical power of 1.6E8 W-silicon from the first pulse and 2.1E8 W-silicon from the second. It triggered and passed all discriminants of an unmodified (EMP requirement excepted) NBDS sensor station at 1 km.

TABLE III

Shot 1 (2/28/78)

		Max 1		Min		Max 2	
Range	Instrument	Ampl	Time	Ampl	Time	Ampl	Time
1 km (Hill 1)	OSS 1 ND 1	1.3×10^{-3} (4P)	2.44 (34 1/2)	2.3×10^{-7} (OA)	97.5 (76 1/2)	1.67×10^{-3} (5B)	359 (91 1/2)
	NBDS 1 D+S	- - -	- - -	- - -	41.9 274.3 kT (225)	- - - NFO	- - -
3.83 km (Pad 1)	OSS 2 ND 2	2.6×10^{-5} (4A)	2.44 (34 1/2)	2.3×10^{-8} (OA)	56.6 (70 1/2)	5.6×10^{-5} (4H)	359 (91 1/2)
4.16 km (Pad 2)	SSO 2 ND 1	4.5×10^{-5} (105)	1.85 (227_8)	3.2×10^{-7} (000)	52.4 (278_8)	9.3×10^{-5} (117)	340 (323_8)
10.51 km (Bldg 802)	OSS 3 ND 1	6.9×10^{-6} (4J)	2.12 (33 1/2)	2.3×10^{-9} (OA)	62.5 (72)	8.6×10^{-6} (4L)	312 (90)

- -

Visibility at: 1 km (Hill 1) ~ 30 km (0.063 V)
10 km (Bldg 880) > 40 km (0.01 V)
24 km (AT&T) > 40 km (0.019 V)

Cloud Deck at 1500 to 2000 ft

NBDS 2 (D+5) and NBDS 3 (S only) did not trigger at Pad 1

SSO 1 did not trigger at AT&T (24 km)

Ampl in W/cm^2-silicon

Time in ms

(c)

(d)

Figure 10. (concluded)

Shot 1

Table III summarizes bhangmeter data obtained from Shot 1. Optical time histories from four line-of-sight detectors at ranges from 1.0 to 10.5 km are plotted in Figure 11. This ELS produced optical power of 1.6E8 W-silicon from the first pulse and 2.1E8 W-silicon from the second. It triggered and passed all discriminants of an unmodified (EMP requirement excepted) NBDS sensor station at 1 km.

TABLE III

Shot 1 (2/28/78)

		Max 1		Min		Max 2	
Range	*Instrument*	*Ampl*	*Time*	*Ampl*	*Time*	*Ampl*	*Time*
1 km (Hill 1)	OSS 1 ND 1	1.3×10^{-3} (4P)	2.44 (34 1/2)	2.3×10^{-7} (OA)	97.5 (76 1/2)	1.67×10^{-3} (5B)	359 (91 1/2)
	NBDS 1 D+S	- - -	- - -	- - -	41.9 274.3 kT (225)	- - - NFO	- - -
3.83 km (Pad 1)	OSS 2 ND 2	2.6×10^{-5} (4A)	2.44 (34 1/2)	2.3×10^{-8} (OA)	56.6 (70 1/2)	6.6×10^{-5} (4H)	359 (91 1/2)
4.16 km (Pad 2)	SSO 2 ND 1	4.5×10^{-5} (105)	1.85 (227_8)	3.2×10^{-7} (000)	52.4 (276_8)	9.3×10^{-5} (117)	340 (323_8)
10.51 km (Bldg 802)	OSS 3 ND 1	6.9×10^{-6} (4J)	2.12 (33 1/2)	2.3×10^{-9} (OA)	62.5 (72)	8.4×10^{-6} (4L)	312 (90)

Visibility at: 1 km (Hill 1) ≈ 30 km (0.063 V)
10 km (Bldg 802) > 40 km (0.01 V)
24 km (AT&T) > 40 km (0.016 V)

Cloud Deck at 1500 to 2000 ft

NBDS 2 (D+S) and NBDS 3 (S only) did not trigger at Pad 1

SSO 1 did not trigger at AT&T (24 km)

Ampl in W/cm^2-silicon

Time in ms

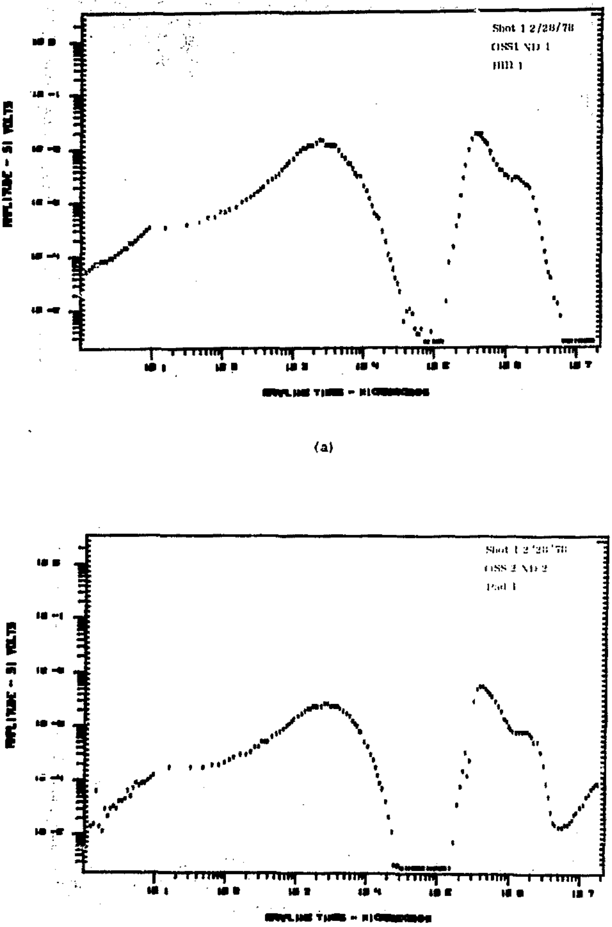

(a)

(b)

Figure 11. Shot 1

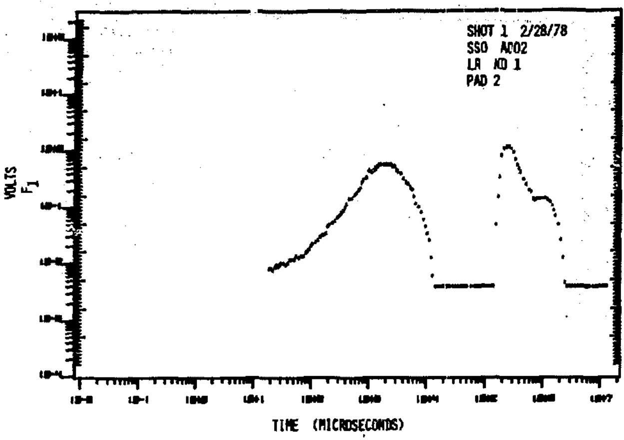

(c)

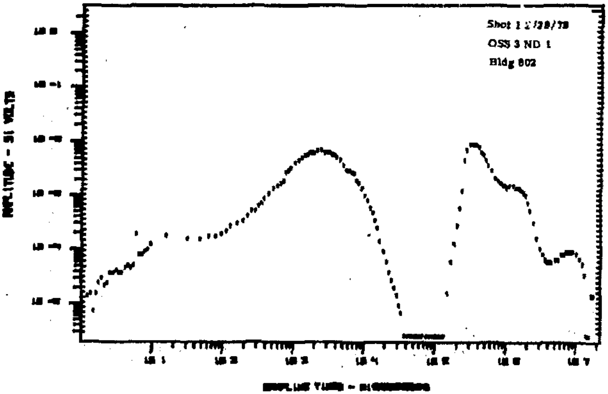

(d)

Figure 11. (concluded)

Shot 2

Bhangmeter data for Shot 2 is summarized in Table IV. Optical time histories from three line-of-sight detectors at ranges from 1.0 to 3.6 km are plotted in Figure 12. This ELS produced optical power of 8.7E7 W-silicon from the first pulse and 1.2E7 W-silicon from the second. The low output and irregular shape of the second pulse was caused by improper ignition on all its bags.

TABLE IV

Shot 2 (3/2/78)

		Max 1		Min		Max 2	
Range	**Instrument**	**Ampl**	**Time**	**Ampl**	**Time**	**Ampl**	**Time**
1 km (Hill 1)	OSS 1 NO ND	6.6×10^{-4} (50)	3.05 (37)	2.8×10^{-6} (2M)	40.0 (86 1/2)	9.7×10^{-5} (4M)	187 (84)
1.73 km (Hill 2)	OSS 2 ND 0.3	1×10^{-4} (7A)	3.17 (37 1/2)	3.7×10^{-7} (3N)	42.9 (67)	1.7×10^{-5} (8A)	179 (83 1/2)
3.6 km (Hill 3)	SSO 2 NO ND	3.4×10^{-5} (141)	2.87 (234_8)	1.2×10^{-7} (23)	39.3 (272_8)	7.5×10^{-6} (114)	183.5 (314_8)

Visibility at: 1 km (Hill 1) - - - -
10 km (Bldg 880) > 40 km (0.008-0.01 V)
15.3 km (Blue Cross) > 40 km (0.019 V)

NBDS 1 (D+S) did not trigger at Hill 1 (1 km)

NBDS 2 (D+S) and NBDS 3 (S only) did not trigger at Hill 2

OSS 3 (NO ND) did not trigger at Bldg 802 (10.5 km)

SSO 1 (NO ND) did not trigger at Blue Cross (15.3 km)

Ampl in W/cm^2-silicon

Time in ms

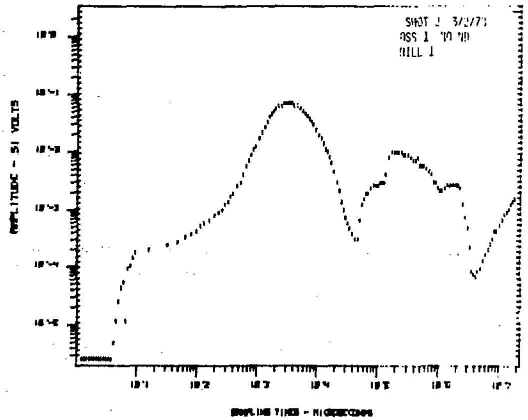

(a)

Figure 12. Shot 2

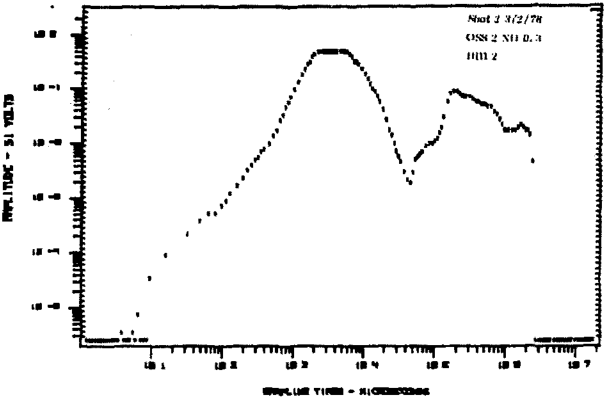

(b)

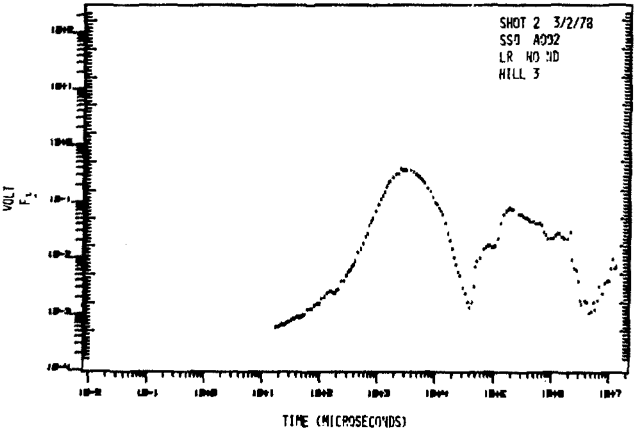

(c)

Figure 12. (concluded)

Shot 3

Bhangmeter data for Shot 3 is summarized in Table V and optical time histories from four line-of-sight detectors at ranges from 1.0 to 3.6 km are plotted in Figure 13. This ELS produced optical power of 1.2E8 W-silicon from the first pulse and 4.1E7 W-silicon from the second. The low output and irregular, two-hump shape of the second pulse was caused by the use of aluminum powder particles of two different sizes which burned at different rates. This shot triggered detectors north, south and east of the source and provided information on directional effects.

TABLE V

Shot 3 (3/3/78)

		Max 1		Min		Max 2	
Range	**Instrument**	**Ampl**	**Time**	**Ampl**	**Time**	**Ampl**	**Time**
1 km (Hill 1)	OSS 1 NO ND	9.7×10^{-4} (6B)	2.93 (36 1/2)	1.2×10^{-5} (5J)	24.3 (60 1/2)	3.2×10^{-4} (5H)	74.1 (73 1/2)
1.26 km (Back side)	SSO 3 ND 1	6.5×10^{-4} (148)	2.87 (234_8)	9.3×10^{-6} (57)	22.8 (264_8)	2.9×10^{-4} (137)	340 (323_8)
1.4 km (Solar Tower)	SSO 1 ND 1	2.6×10^{-4} (135)	2.87 (234_8)	4.2×10^{-6} (44)	22.9 (264_8)	1.3×10^{-4} (124)	78.6 (302_8)
3.6 km (Hill 3)	OSS 2 ND 1	5×10^{-5} (9L)	2.57 (35)	9.7×10^{-7} (3H)	21.4 (69)	2.3×10^{-5} (5E)	81.9 (74 1/2)

Visibility at 1 km (Hill 1) = 18-19 km (0.10 - 0.11 V)
~1.6 km (Solar Tower) > 40 km (0.022 V)
10 km (Bldg 880) > 40 km (0.03 - 0.05 V)

Nephelometer at ~1.6 km (Solar Tower) 0.9×10^{-4} scattering coef.
0.5×10^{-4} with heater
(~50 mile or 80 km visibility)

NBDS 2 (O&S) and NBDS 3 (S only) did not trigger at Hill 1

OSS 3 (NO ND) did not trigger at Bldg 802 (10.5 km)

NBDS 1 was not fielded.

Ampl in W/cm^2 - silicon

Time in ms

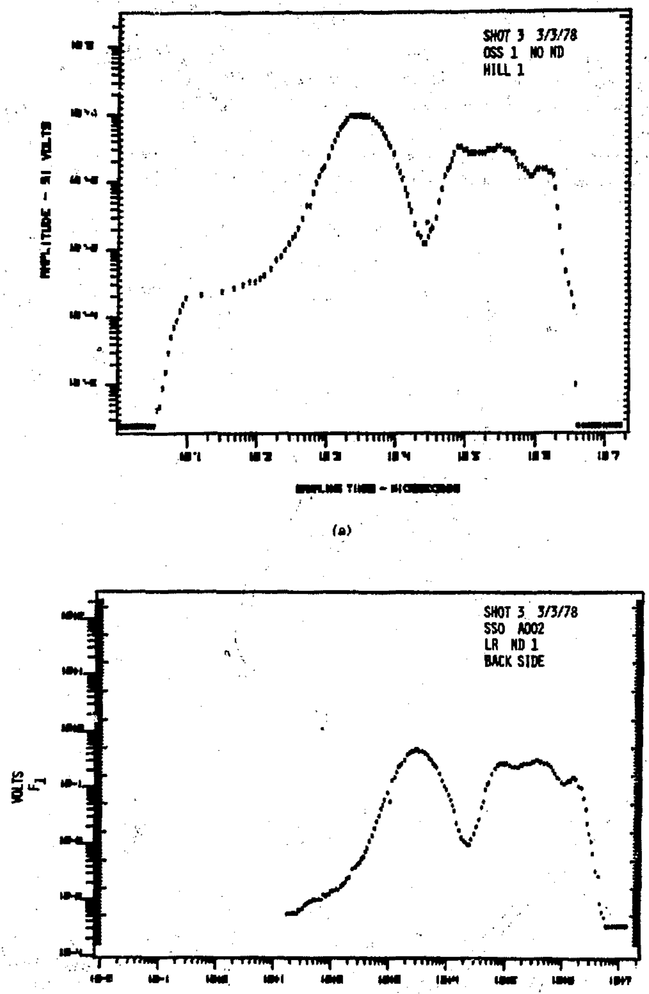

(a)

(b)

Figure 13. Shot 3

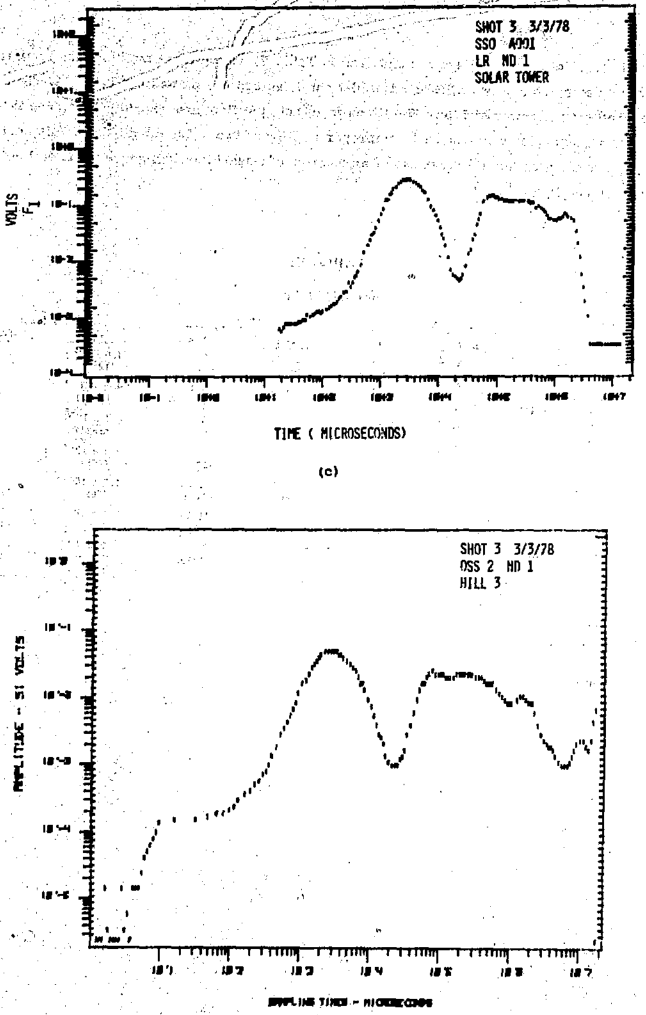

(c)

(d)

Figure 13. (concluded)

Shot 4

Bhangmeter data for Shot 4 is summarized in Table VI and optical time histories from five line-of-sight detectors and two NBDS scattered-light detectors are plotted in Figure 14. This ELS produced optical power of 1.5E8 W-silicon from both the first and second pulse. The irregular shape of the second pulse was caused by improper ignition of two of the eight bags. This shot provided information on the effectiveness of attenuation of flash-blindness goggles and on line-of-sight vs scattered light.

TABLE VI

Shot 4 (3/7/78)

Range	Instrument	Max 1		Min		Max 2	
		Ampl	Time	Ampl	Time	Ampl	Time
~300 m (Bldg 9965)	OSS 1 ND 1.0	1.1×10^{-2} (142_8)	2.93 (36 1/2)	2.1×10^{-5} (51_8)	37 (65 1/2)	4.0×10^{-3} (131_8)	343 (01)
	OSS 2 ND 2 Passive Goggle	1.5×10^{-3} (145_8)	2.57 (35)	2.3×10^{-6} (52_8)	33.1 (64 1/2)	4.5×10^{-4} (132_8)	260 (88)
	OSS 3 NO ND "Dark Goggle"	6.2×10^{-5} (162_8)	2.81 (36)	1.1×10^{-7} (70_8)	35 (65)	2.6×10^{-5} (152_8)	250 (88)
1 km (Hill 1)	SSC 1 ND 1	1.2×10^{-3} (162)	2.87 (234_8)	2.5×10^{-6} (35)	36 (271_8)	1.2×10^{-3} (163)	288 (320_8)
	NBDS 2 Rate + 10	1.2×10^{-5} (79)	2.08 (93)	8.6×10^{-8} (00)	31.04 (209)	1.2×10^{-5} (30)	263.8 (311 1/2)
	NBDS 3 Rate + 5	2.8×10^{-5} (98)	2.2 (95)	8.0×10^{-8} (00)	31.04 (209)	2.8×10^{-5} (98)	278.7 (310 1/2)
3.6 km (Hill 3)	SSO 2 NO ND	5.6×10^{-5} (147)	2.87 (234_8)	8.1×10^{-8} (15)	36 (271_8)	6.0×10^{-5} (151)	288 (320_8)

Visibility at: 1 km (Hill 1) ≈ 19 km (0.1 V)
10 km (Bldg 880) > 40 km (0.013 V)

Ampl in W/cm^2 - silicon

Time in ms

NBDS 1 was not fielded

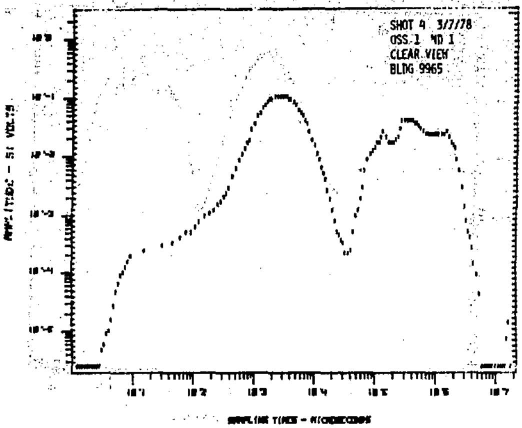

(a)

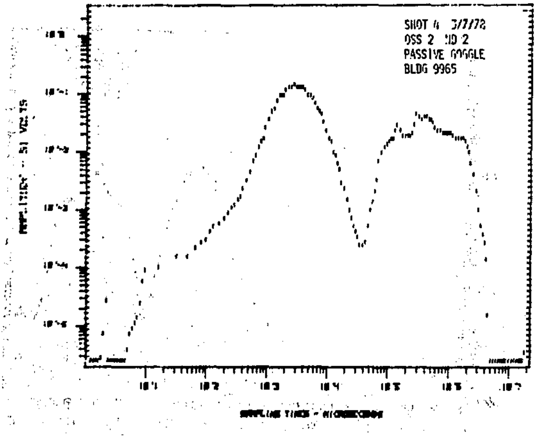

(b)

Figure 14. Shot 4

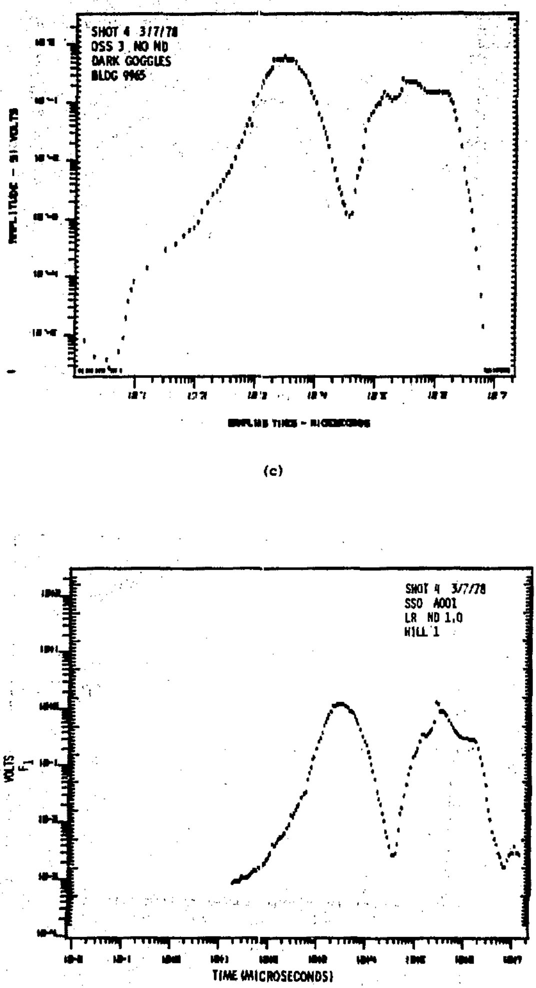

(c)

(d)

Figure 14. (cont)

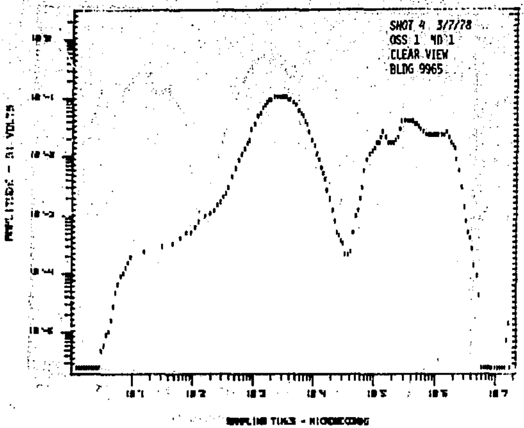

(a)

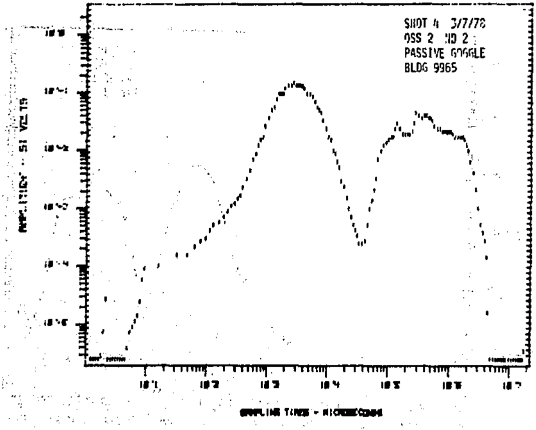

(b)

Figure 14. Shot 4

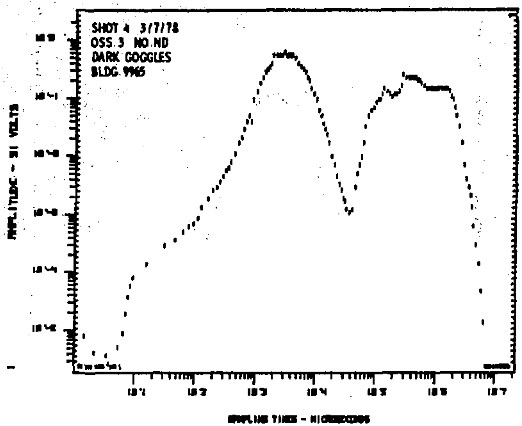

(c)

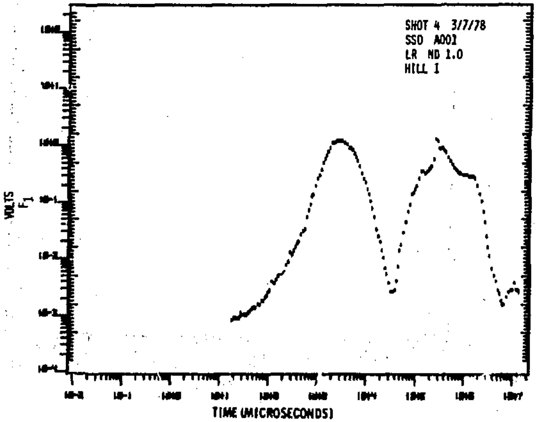

(d)

Figure 14. (cont)

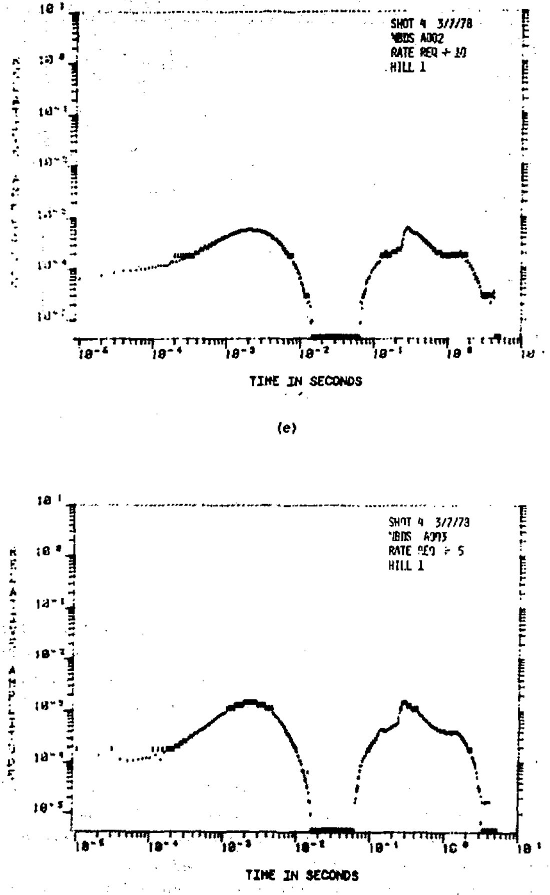

(e)

(f)

Figure 14. (cont)

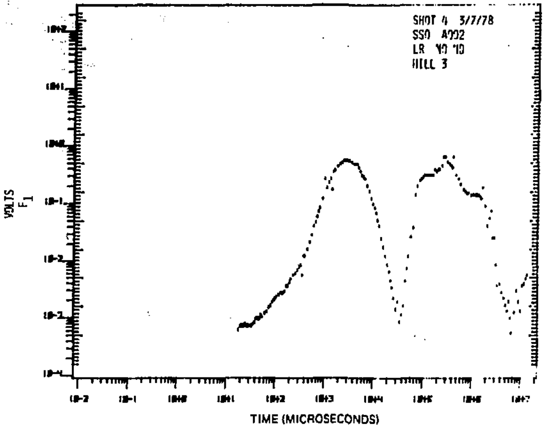

(g)

Figure 14. (concluded)

Conclusions

Various conclusions concerning optical transmission, the ELS, and the detectors are detailed in the following paragraphs. Overall, the ELS proved to be a safe, usable, low-cost device for optical measurements. It has a high potential value for training troops and for demonstrating simulated optical and thermal nuclear effects without radiation or blast.

Optical Transmission

Figure 15 is a plot of irradiance at first maximum as a factor of range for the 13 measurements using the direct (line-of-sight) detectors. The data and the transmission loss curves have been normalized at 1 km to adjust for any variation in source output. The data points indicate a $1/R^2$ dependence within a factor of two. Improvement is not significant enough to justify the more complex Monte Carlo scattering model. This plot is for clear air (65-km visibility) to a range of 10.5 km. Treating the ELS as a point source, $4\pi R^2$ radiator, appears justified under these conditions.

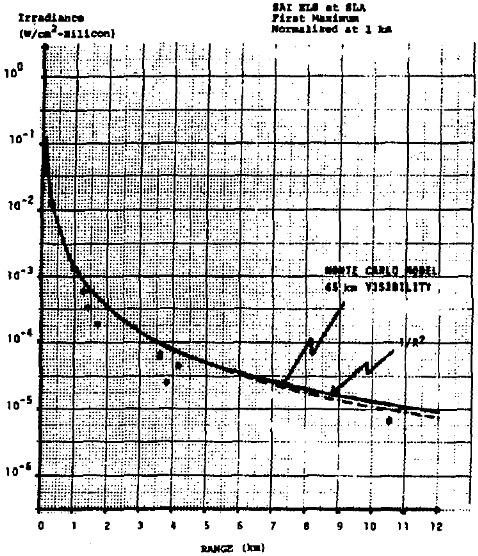

Figure 15. Plot of Irradiance at First Maximum

Direct vs Scattered Ratio and Shape

Table VII lists data from Shot 4 at 1 km. Comparing the SSO direct line-of-sight measurement (Figure 14d) with the NBDS scattered-light measurements (Figures 14e and 14f) indicates an excellent waveshape match and a direct/scattered ratio of 45 to 100 for the conditions. The cause of spread in the ratio has not been determined and is especially surprising when the different requirements of the relaxed rate of rise trigger for the NBDS stations are considered. Possible differences in leveling or in sensitivity to direct component light in the tail of the field-of-view may be the cause. In any case, an estimate for the short-range, clear-air direct and scattered ratio has been achieved and preservation of scattered light waveshape has been demonstrated.

TABLE VII

Direct Scattered Ratio

Shot 4 at 1 km

Direct	SSO 1 ND 1	1.2E-3 W/cm^2-Silicon
Scattered*	NBDS 2 Rate + 10	1.2E-5 W/cm^2-Silicon
Scattered*	NBDS 1 Rate + 5	2.8E-5 W/cm^2-Silicon

Direct/Scattered Ratio ≈ 45 to 100 Clear Air 1 km

---

*May include ≤ 1% direct component

Nuclear Optical Simulator

The Nuclear Burst Detection System (NBDS) was triggered on two ELS shot. A sensor station equipped with full optical discriminants,* 1 km from Shot 1, automatically processed the ELS signature and reported a 274-kt nonfallout (NFO) producing nuclear event. Unfortunately, failure of the communication link resulted in loss of the time history record from this sensor. On Shot 4, at 1 km, two NBDS stations using special nondiscriminant software and relaxed optical rate-of-rise requirements recorded the ELS time history. When the optical waveshape discriminants which NBDS uses to define a nuclear event (Table VIII) were applied manually, they indicated that this ELS would have been reported as a 68.5-kt fallout (FO) producing nuclear burst. Other NBDS measurements were attempted but failed because of inadequate ELS rate-of-rise at the given ranges (see next paragraph). Below is a summary of results garnered from applying the NBDS software discriminants to the measured ELS signatures, demonstrating that an ELS of this type can meet present NBDS optical discriminants and can be used to simulate nuclear optical effects:

- Shot 1 - An NBDS sensor station equipped with a full set of optical discriminants (hardwire and microprocessor), but without EMP requirements, automatically reported a 274-kt NFO event.

- Shot 2 - Manually applying microprocessor discriminants to the recorded time history of line-of-sight detectors (OSS) indicated that a 246-kt NFO event would have been reported.

- Shot 3 - Manually applying discriminants to the recorded time history of direct detector (OSS) indicated failure to pass discriminant No 5 because of irregular second pulse.

---

*All NBDS sensor station had Electromagnetic Pulse (EMP) requirements disabled.

- *Shot 4 - This shot triggered the NBDS sensor station with* relaxed rate-of-rise optical requirements and disabled EMP requirements. Manually applying microprocessor discriminants to the recorded time history of the NBDS indicated that a 68.5-kt FO event would have been reported.

TABLE VIII

NBDS

Microprocessor Discriminants

1. First Sample > 6.3×10^{-7} W/cm^2 (LD 32)
2. First Peak Time < 3.6 ms (Sample 113)
3. Time of (First Peak Amplitude ÷ 6.25) > 0.5 ms (Sample 41)
4. 5 x First Peak Time < Minimum Time < 70 x First Peak Time
5. 4 x Minimum Time < Second Peak Time < 20 x Minimum Time
6. Minimum Time < 189 ms (Sample 295)
7. Minimum Width < 8 x Minimum Time
   (< 96 Samples at Same Level Detector (LD) Before 102 ms (Sample 264))
8. At Least One Third of Samples (88) Before 100 ms (Sample 264)
   > (First Peak Amplitude ÷ 6.25)
9. Single Peak Pulses are Rejected (Second Peak Start Before
   1800 ms (Sample 396))
10. Flat First Peak Pulses of Long Duration are Rejected (First Peak Amplitude > Avg Amplitude of Up to 128 Samples)
11. (Second Peak Amplitude ÷ 6.25) > Amplitude of Minimum
12. All Samples Between Second Peak and 10 Samples Past Second Peak > (Second Peak Amplitude ÷ Approximately 6.25/3 (1.36 to 2.64) (Peak Level Detector (LD-10))

<u>First Pulse Rate of Rise</u>

To reduce false triggering, bhangmeters designed to detect nuclear bursts use ac-coupled trigger circuitry consistent with nuclear optical rise times. Because of this requirement, the characteristic that most limited the range at which the ELS could be detected was the rate-of-rise of the first pulse. Table IX presents the ELS rate of rise determined by two methods: the average rate, determined from the first peak amplitude/time ratio, and the initial rate from the presamples of Old Style Suitcase measurements. Comparing the methods indicates that the initial rate of rise is slower by a factor of 10 to 100, than the average rate. This is particularly troublesome because background compensation circuitry in the bhangmeter will compensate out the signal until it exceeds the trigger rate-of-rise requirement, thus resulting in late triggering and reduced amplitude. Comparing the measured rise times with the trigger requirements listed in Table IX confirms the inability to trigger the NBDS beyond 1 km or a direct bhangmeter beyond 10.5 km. This is *further verified by the fact that the source was strong enough* to be seen and recorded on movie film at over 25 km.

TABLE IX

First Pulse Rate of Rise

Measurements:

Method	Rate of Rise 10 km to 300 m (W/cm^2-s)	Rate of Rise Source (W/s)
Peak Amplitude Time (Average Rate)	3.3E-3 to 3.8	1.2E10 to 6.7E10
OSS Presamples (Initial Rate)	3.1E-4 to 8E-2	1.2E8 to 9.6E9

Requirements:

	Rate of Rise at Detector (W/cm^2-s)		Rate of Rise Source (W/s)	
	Direct	NBDS	Direct	NBDS
10 km Trigger	3.1E-4	1.3E-2	3.9E8	3.2E12*
1 km Trigger	3.1E-4	1.3E-2	3.9E7	1.6E11*

Conclusion:

ELS as Detonated at SLA Has Slow Rise Compared to Bhangmeter Requirements Which are Designed to Detect Nuclear Bursts

---

*Assumes direct scattered factor of 20 at 10 km, 100 at 1 km.

Second Pulse Shape

There was considerable variation in the shape of the second pulses. The first shot went approximately as predicted from single bag tests. The second and fourth shots produced lower amplitude than expected and showed irregularly shaped maximums because of improper ignition on all or some of the eight bags. Late ignition was confirmed from high-speed (1500 ft/s) movies of the events. Shot 3 resulted in a low, two-peaked shape caused by aluminum powder made of a mixture of particles of two different sizes which burned at different rates. Comparing the smoothness and consistency of the 64-point first pulses to the 8-bag second pulses indicates that there is an advantage to using multipoint sources because a malfunction of a part which is a small percentage of the whole would not greatly affect the results.

Source Symmetry

Table X lists the measurements made from three directions from Shot 3. Comparing the estimated source strengths (calculated by folding back using $4\pi R^2$) indicates, to within a factor of two, that both first and second pulse units are nondirectional. Also, there is only negligible transmission loss of output of the first pulse through the bags of the second pulse.

TABLE X

Source Symmetry

Shot 3 (3/3/78)

Range (km)	Direction (Approx)	Instrument	Max 1		Max 2	
			Signal (W/cm^2-Silicon)	Source Strength (W-Silicon)	Signal (W/cm^2-Silicon)	Source Strength (W-Silicon)
1.0 (HDD 1)	North	OSS 1 NO ND	9.7E-4	1.22E8	3.2E-4	4.0E7
1.26 (Back Side)	South	SSD 2 ND 1	4.5E-4	8.38E7	2.9E-4	5.8E7
1.4 (Solar Tower)	East	SSD 1 ND 1	2.6E-4	6.4E7	1.3E-4	3.2E7

Conclusions: 1) Within Factor of 2, Source is Nondirectional.

2) Transmission Loss of First Pulse Through Second Pulse Bags is Negligible.

Output and Yield Scaling

Table XI lists the optical source strengths of the four ELS shots. The first-pulse units averaged 1.3E8 W-silicon and the Shot 1 second-pulse unit achieved 2.1E8 W-silicon (see above concerning Shots 2, 3, and 4 second pulse). For comparison, the table also lists source strengths of various other events. Considering the small quantity of explosive (approximately 150 g) and the low cost of an ELS, the optical output advantages are considerable.

TABLE XI

ELS Output

Shot No	First Pulse* (64 Points)	Second Pulse* (8 Bags)
1	1.6E8	2.1E8
2	8.7E7	1.2E7
3	1.2E8	4.0E7
4	1.5E8	1.5E8

---

*Source Strength in W-Silicon Calculated From Measurement at 1 km.

Other Sources*

Nuclear Burst	Second Maximum (1 kt)	1.8E13
Dice Throw	630 Tons ANFO	1.2E10
Predice Throw II	120 Tons ANFO	7.1E9
Lightning	Return Strokes	1E8 to 1E12

---

*Source Strengths in W-Silicon

Table XII summarizes calculations of optical output and yield for second-pulse units. The source strength scales as approximately the number of bags to the two-third power. If this scaling law is used, the output of the 40-bag shots to be made at Fort Ord is expected to be 8.2E8 W-silicon.

TABLE XII

Yield Scaling

Yield	Method	Source Strength -Silicon)
1 Bag	Average of 6 Shots	6.98E7
8 Bag	Linear Scaling	5.6E8
	$(\text{YIELD})^{2/3}$ Scaling	2.8E8
	Shot 1 at SLA	2.1E8
40 Bag	$(\text{YIELD})^{2/3}$ Scaling	8.2E8

Conclusion: Optical Source Strength Increases as Approximately $(\text{YIELD})^{2/3}$

References

1. Development of a Large Scale Thermal Radiation Simulator, SAI-77-528-SV (Final Report; Sunnyvale: Science Applications Inc, 30 November 1977).
2. R. G. Bradley et al, Super Suitcase Optical: Operations Manual, Vol. 1 (Albuquerque: Sandia Laboratories, 1974).

APPENDIX

Data Available From and Participants in ELS Shots Conducted at Sandia Laboratories

Data Available From
SAI ELS/Thermal Tests at SLA

Data Type	Organization	Shot(s)	Range(s)	Description
Calorimeter (Q vs Time)	NWEF (Pete Hughes)	1,2,3,4	3.5 m, 4.5 m, 5.5 m south of "C" sys.	3000-Hz Circular Foil Heat Flux Gages
Source Strength (Thermal)	SLA-9337 (Ned Keltner)	1,2,3,4	4.0 m south of "C" sys.	2 Circular-Foil Gages 1 Silicon-Diode Sensor
Optical Signal (Suns vs Time)	SAI (Jerry Lattery)	1,2,3,4	200 ft north of "C" sys.	Photodiode Oscilloscope
Optical Signal	SLA-9412 (Dale Fastle)	2,3	~300 m north	Diode
Optical Signal (W/cm^2 vs Time)	SLA-1245 (Ron Glaser)	1,2,3,4	300 m to 10.5 km north, south, & east	Silicon Diode Bhangmeters
Photometrics (1500 f/s)	SLA-9412 (Terry Leighley)	1	90 ft north of "C"	Passive Goggle
		2	east & west	Materials (6 cameras)
		2	5.5 m south of "C"	Active & Passive Goggle
		2	90 ft north of "C"	Active & Passive Goggle
		2	east & west	Materials (6 cameras)
		3	5.5 m south of "C"	Active & Passive Goggle
		3	90 ft north of "C"	Active Goggle
		3	east & west	Materials (6 cameras)
		4	90 ft north of "C"	Passive Goggle
		4	east & west	At Bags (2 cameras)
(400-500 ft/s)	SLA-9412 (Terry Leighley)	3,4	north, east, south	Overall Views
		4	~300 m north	Active & Passive Goggle
Documentary (Motion Picture)	SLA-3153 (Gene Moore)	1,2,3,4	GZ and 1 km	All Aspects
	SLA-1245 (Dean Thornbrough)	1,2,3,4	1 km	Shots, Visitors Bhangmeter Setup
	SLA-1245 (Fred Bauer)	1,2,3,4	1.26 km to 25 km	Bhangmeter Mounted (2 locations shot)

Data Type	Organization	Shot(s)	Range(s)	Description
Documentary (Stills)	SLA-9412 (Terry Leighley)	2,3	GZ and 1 km	All aspects (33 color)
	SLA-3162 (Russell Smith)	3	GZ and 1 km	Shot Sequence (14 B&W)
	SAI			
	(John Dishon)	1,2,3,4	GZ	All aspects
	(Wilson North)	2	GZ and 1 km	All aspects
Documentary (Slides)	NWEF (Pete Hughes)	2,3	GZ	Materials (80 before and after)
Microbaragraph	SAI (SLA-1132) (Mike McDonnel)	3,4	1 km	Overpressure vs Time
Impact Noise	SLA-3311 (Bill Stocum)	4	1 km	Peak pressure
Nephelometer	SAI (SLA-5713) (Mike McDonnel)	3,4	1.6 km	Scattering Coef. (with/without heater)
Visibility (Weather)	SLA-1245 (Ron Glaser)	1,2,3,4	1 km to 25 km	Visiometer Airport weather